From enhanced to reduced quantum antiferromagnetism by tuning a magnetic impurity

Julian Engel and Stefan Wessel
Institut für Theoretische Physik III, Universität Stuttgart, Pfaffenwaldring 57, 70550 Stuttgart, Germany
(Received 16 March 2009; revised manuscript received 11 August 2009; published 9 September 2009)

Based on quantum Monte Carlo simulations, we study the local-order-parameter modulations induced by a magnetic impurity that couples to a single moment of a two-dimensional quantum antiferromagnet. A strong antiferromagnetic coupling of the impurity spin reduces the antiferromagnetic order in the host beyond the next-nearest-neighbor sites of the impurity spin, whereas on the next-nearest neighbors the order increases, similar as for an embedded vacancy. We show that for weak and intermediate couplings to the impurity spin, the local antiferromagnetic order is enhanced throughout the host magnet. We compare our numerical findings to analytical results from a recent perturbative approach based on spin-wave theory.

DOI: 10.1103/PhysRevB.80.094404 PACS number(s): 75.10.Jm, 75.30.Hx, 75.40.Mg

I. INTRODUCTION

The effects of impurities on the properties of magnets have been the subject of intensive investigations since many years. One reason for this effort is the fact that impurities are essentially present in all magnetic materials. Furthermore, systematically studying the response of a magnetic system to impurities of known kind provides an important means of probing the system's properties. Examples of such studies include the effects of dilute magnetic impurities in quantum antiferromagnets. This situation is similar to the Kondo problem of a magnetic impurity that couples to the host electrons of a metal.[1,2]

In the past years, various theoretical studies discussed the effects of a single magnetic impurity in a low-dimensional antiferromagnet, in particular on the square lattice.[1–12] The scenario under consideration here is illustrated in Fig. 1 and consists of a square lattice of localized spin-$\frac{1}{2}$ moments with an antiferromagnetic nearest-neighbor Heisenberg exchange J, plus a localized impurity spin-$\frac{1}{2}$ degree of freedom, connected via a different antiferromagnetic exchange coupling J' to a single site in the host magnet. Denoting the host spin on lattice site i by $\mathbf{S}_i$ and the impurity spin by $\mathbf{s}$, the Hamiltonian describing this system is given by

$$H = J\sum_{\langle i,j\rangle} \mathbf{S}_i \cdot \mathbf{S}_j + J'\mathbf{S}_0 \cdot \mathbf{s}. \tag{1}$$

In the absence of J', the ground state of the host magnet is well known to exhibit long-ranged antiferromagnetic order, with a staggered magnetization that is reduced by quantum fluctuations from the classical Néel state value of 1/2 down to a value of about $m_s = 0.307$.[13–15]

For large impurity coupling $J' \gg J$, the dominant tendency toward singlet formation along the J' bond between the host spin $\mathbf{S}_0$ and the impurity site $\mathbf{s}$ leads to an effective decoupling of the host spin and the impurity site from the rest of the system.[6] In the strong-coupling limit $J'/J \to \infty$, this local singlet formation leaves behind an effectively depleted host system, as if the spin $\mathbf{S}_0$ had been removed. For sufficiently large values of J', one thus expects to recover within the host magnet a similar behavior as in case of a static vacancy in the host. Due to the reduced connectivity next to the impurity site (the local coordination number being reduced from $z=4$ in the clean case to $z=3$), the staggered magnetization gets enhanced at the nearest-neighbor sites to the missing spin, while the antiferromagnetic order decreases throughout the reminder of the host in this inhomogeneous antiferromagnetically ordered system.[16–18] The enhanced order at the low-coordinated site in case of a static vacancy fits well within a general trend in inhomogeneous quantum antiferromagnets, where the staggered magnetization tends to decrease with increasing local coordination number z.[19,20] For weak to intermediate coupling $J' \lesssim J$, the tendency toward the host-impurity singlet formation competes with an alignment of the impurity spin to the existing antiferromagnetic background in the host. Previous studies,[3,12] based on improved spin-wave theories, suggest that one would indeed expect to find an enhancement of the antiferromagnetic order throughout the whole host system for weak to intermediate values of $J' \lesssim J$. Here, we consider this situation using unbiased quantum Monte Carlo simulations in order to analyze the expected crossover from a globally enhanced antiferromagnetism at weak impurity coupling to the limiting strong-coupling local singlet formation. The paper is organized as follows. In Sec. II, we discuss our numerical approach to measure the local antiferromagnetic order parameter and present in Sec. III our findings on the position-resolved staggered magnetization and the spin-spin correlations. We then compare our numerical results to the analytical prediction of Ref. 12. We conclude in Sec. IV with a summary of our findings and an outlook toward future investigations.

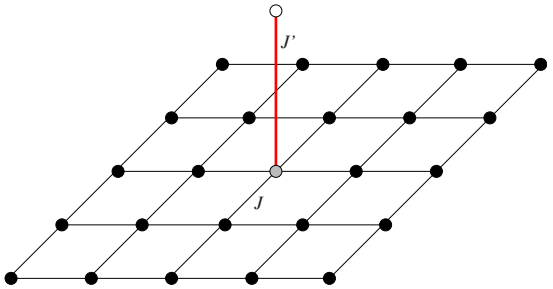

FIG. 1. (Color online) Illustration of a lattice of spin-$\frac{1}{2}$ moments localized on a square lattice (black and gray circles) with nearest-neighbor exchange J, plus an additional impurity spin (white circle), coupled via exchange J' to a single binding site (gray circle) of the host.

II. METHOD

A standard way of measuring the value of the staggered magnetization in an (inhomogeneous) quantum antiferromagnet employs the infinite system expectation value of the spin operator, applying an infinitesimally small symmetry breaking field. For the current consideration, this leads to the expression

$$m_s(i) = \lim_{h\to 0} \lim_{N\to\infty} \frac{\mathrm{Tr}(S_i^z e^{-\beta(H-hO_{\mathrm{AF}}^z)})}{\mathrm{Tr}\, e^{-\beta(H-hO_{\mathrm{AF}}^z)}} \tag{2}$$

for the local staggered magnetization. Here, $\beta=1/T$ denotes the inverse temperature ($k_B=1$) and

$$O_{\mathrm{AF}}^z = \sum_i \epsilon_i S_i^z, \tag{3}$$

with $\epsilon_i=\pm 1$ depending on the sublattice to which lattice site i belongs. Due to the $SU(2)$ symmetry of H, the same result is obtained if instead of the z component, the x or y component is considered. In case of a uniform system, such as, e.g., the square lattice at $J'=0$, the resulting value is independent of the lattice site, $m_s(i)=m_s$, and defines the staggered magnetization m_s of the system. While such an approach is often taken in exact and approximate analytical calculations, it requires knowledge of two extrapolation formulas if based on numerical data, e.g., from quantum Monte Carlo (QMC) simulations, where only finite systems can be studied. One would need to obtain for a given small value of h various finite-size expectation values, extrapolate them to the thermodynamic limit, and eventually take the limit of $h\to 0$ on the extrapolated values. Thus in most numerical simulations instead, the staggered magnetization of a uniform antiferromagnet is defined in the absence of a symmetry-breaking field ($h=0$), based on the spin-spin correlations in $\langle (O_{\mathrm{AF}}^z/N)^2\rangle$ that is dominated by the correlation function $\langle \mathbf{S}_i\cdot\mathbf{S}_j\rangle$ at large distances.[13,14] The long-range order parameter σ is obtained upon performing a single extrapolation

$$\sigma^2 = \lim_{N\to\infty} \langle (O_{\mathrm{AF}}^z/N)^2\rangle \tag{4}$$

using a polynomial in $1/\sqrt{N}$.[13,14] It is generally accepted that the two approaches are equivalent, in that $m_s=\sqrt{3}\sigma$ [the factor $\sqrt{3}$ being related to the $SU(2)$ symmetry of H]. While this expectation holds if the system is assumed to obey a pure state decomposition[21,22] (which is usually considered to be the case), a strict proof of the above equality is still lacking (however, it has been proven[21,22] that $m_s\geq\sqrt{3}\sigma$, so that σ provides a lower bound on m_s). Note, that the currently most precise estimate[15] of the staggered magnetization in the uniform Heisenberg model on the square lattice is based on the estimator in Eq. (4).

To probe the position dependent order parameter in an inhomogeneous quantum antiferromagnet, such as the one shown in Fig. 1, we consider the order parameter from the uniform case and define

$$\sigma(i) = \lim_{N\to\infty} \langle \epsilon_i S_i^z O_{\mathrm{AF}}^z/N\rangle/\sigma. \tag{5}$$

Assuming as in the uniform case a pure state decomposition, we obtain the local staggered magnetization at lattice site i from

$$m_s(i) = \sqrt{3}\sigma(i) \tag{6}$$

since then $\sigma(i)=\langle \epsilon_i S_i^z\rangle\langle O_{\mathrm{AF}}^z/N\rangle/\sigma=[m_s(i)/\sqrt{3}]m_s/m_s$. For a homogeneous system such as, e.g., the square lattice at $J'=0$, this leads to a homogeneous value of the antiferromagnetic order parameter, whereas in the inhomogeneous case, local variations in $m_s(i)$ arise due to the nonuniform support of the magnetic excitations.[20,23] Note, that in all cases, the mean value $(1/N)\Sigma_i m_s(i)=\sqrt{3}\sigma=m_s$, as expected.

In order to explore inhomogeneous magnetic textures near a magnetic impurity, we employ quantum Monte Carlo simulations using the deterministic version of the operator-loop stochastic series-expansion algorithm,[24,25] which performs optimal for this $SU(2)$ invariant problem. We employed finite lattices of L^2+1 spins, with linear system sizes of up to $L=24$, using periodic boundary conditions. As the anticipated changes in the local distribution of the order parameter are small (in many cases, below the percent level), we had to allow for a sufficiently large number of Monte Carlo steps (typically 10^8 measurement steps were employed) in order to obtain significant results. We performed the simulations at a temperature $T=0.01\ J$, sufficiently low to ensure that data is effectively obtained for the ground state of the employed finite systems. Before considering a nonzero value of J', we compared the results from our simulation code to the data for the clean case in Ref. 14 and found perfect agreement within the statistical error bars. In the following section, we discuss in detail our numerical findings for $J'>0$. Besides the local-order parameter, we also measured in our quantum Monte Carlo simulations the spin-spin correlation function

$$C_{i,j} = |\langle \mathbf{S}_i\cdot\mathbf{S}_j\rangle| \tag{7}$$

between two spins on sites i and j. In Sec. III, we present our numerical findings on the above observables.

III. RESULTS

In the analysis, we take into account the residual lattice symmetry around the impurity site and label the position of site i within the host by its radial distance r from the binding site of the impurity spin. The host spin that couples directly to the impurity is thus located at position $r=0$. In Fig. 2, we plot the distance-dependent values of the local staggered magnetization $m_s(r)$ in the vicinity of the impurity spin for various values of the relative impurity coupling strength J'/J. The values have been normalized to the uniform staggered magnetization $m_s^{(0)}$ of the clean ($J'=0$) lattice for the same system size, $L=24$. The plot exhibits the different behavior observed for weak to intermediate coupling (here, $J'/J=0.1$ and $J'/J=1$) and for strong coupling ($J'/J=5$ and $J'/J\to\infty$). In the former case, the data exhibit an overall enhancement of the staggered magnetization around the impurity spin, whereas in the later case, this enhancement is

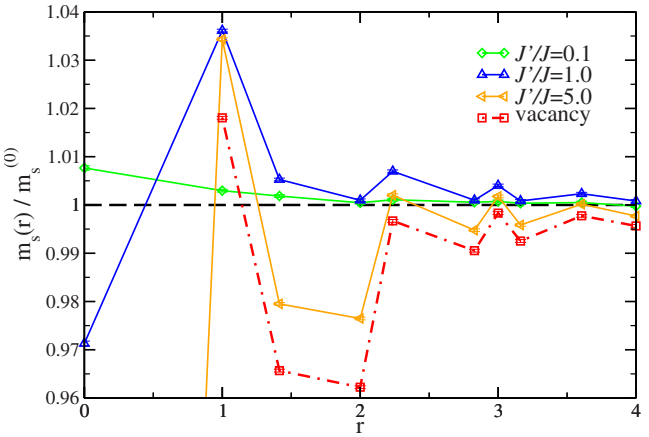

FIG. 2. (Color online) Local staggered magnetization $m_s(r)$ from quantum Monte Carlo as a function of the distance r from the impurity binding site for different values of the relative impurity coupling strength J'/J. Also shown are data for the case of a nonmagnetic impurity (vacancy) corresponding to $J'/J \to \infty$. Horizontal line denotes the reference value of the clean host system.

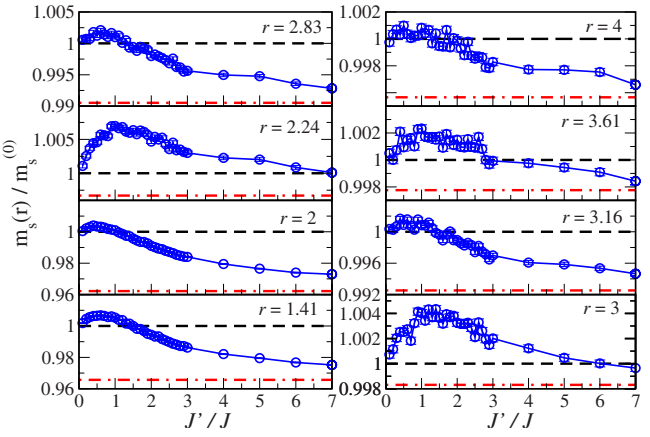

FIG. 4. (Color online) Local staggered magnetization $m_s(r)$ from quantum Monte Carlo as a function of J'/J for various distances r from the impurity binding site. Dashed horizontal lines denote reference values of the clean host system and the dotted-dashed lines represent the limiting values for $J'/J \to \infty$, corresponding to a nonmagnetic impurity (vacancy).

restricted to the nearest-neighbor sites at $r=1$. Furthermore, for $J'/J=0.1$ also $m_s(r=0)$ is enhanced, whereas for $J'/J=1$, it is already suppressed with respect to the clean case.

A spatial representation of the local-order-parameter distribution is shown for $J'/J=1$ and the vacancy limit in the left and right panels of Fig. 3, respectively. Here, the size of the circles corresponds in a linear scaling to the local staggered magnetization at the corresponding lattice site. In addition, we plot along the bonds of the square lattice the strength of the nearest-neighbor spin correlations $C_{i,j}$ using a linear scaling of the line thickness with the bond strength. We employed the same scalings in both panels so that one can also compare relative changes between the two cases. From Fig. 3, the enhanced local staggered magnetization next to the impurity binding site ($r=1$) is clearly identified,

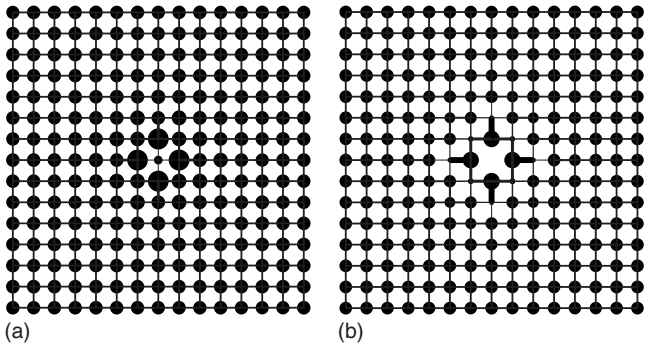

FIG. 3. Local staggered magnetization $m_s(i)$ (represented by the circle radius) and spin-spin correlation function $C_{i,j}$ along the bonds of the host lattice (represented by the line thickness) from quantum Monte Carlo simulations for $J'/J=1$ (left panel) and in the vacancy limit (right panel). The circle radius at site i is linear in $m_s(i)$ [it is proportional to $[m_s(i)/m_s^{(0)}-0.96]/(1.08-0.96)$] in order to make the mild variations in $m_s(i)$ visible in the plot. Similarly, the line thickness is linear in $C_{i,j}$ and is taken proportional to $(C_{i,j}-0.32)/(0.38-0.32)$, again to make the mild variations visible.

as well as the strong suppression in the vacancy limit of $m_s(i)$ for sites coupled directly to those at $r=1$ (i.e., for $r=\sqrt{2}$ and $r=2$, compare to Fig. 2). Concerning the bond strengths $C_{i,j}$, we find for $J'/J=1$ a strong suppression along the bonds connecting the impurity binding site to its neighbors, as expected from the tendency toward the formation of a local singlet between the impurity spin and the binding site. In the vacancy limit, increased bond strengths are found along the bonds linked to sites at $r=1$ that show an increased local staggered magnetization. Apart from this local enhancement, we do not observe any extended valence bond solid (VBS) pattern in the bond strength, such as recently reported in Ref. 26 on the vacancy case. In that study, however, an extended Hamiltonian was examined, which in addition to the two-spin exchange includes strong four-spin interactions that drive the system close to a quantum phase transition between the Néel phase and a VBS regime.[26]

In order to follow more closely the behavior of the staggered magnetization as a function of J'/J, we show in Fig. 4 the coupling dependence for distances r between $\sqrt{2}$ and 4. The corresponding curves for $r=0$, $r=1$, and more details for $r=\sqrt{2}$ and $r=2$ are shown in Figs. 5–8, respectively. We find in all cases that for sufficiently low values of J', the local staggered magnetization is enhanced with respect to the clean case. While for some values of r, this enhancement is observed up to rather large values of J' (e.g., for $J'/J<6$ at $r=\sqrt{5}\approx 2.24$ and $r=3$ in Fig. 4), it is typically restricted to the region $J' \lesssim J$ for the range of distances considered. While on the system sizes studied here, larger distances from the impurity site are available, the changes in the staggered magnetization were too weak as compared to the statistical noise, in order to allow for a similar reliable analysis as for the data shown above. Furthermore, we also found the system-size dependence of the normalized values $[m_s(r)/m_s^{(0)}]$ too weak as compared to the statistical noise in order to perform a reliable finite-size analysis. We thus restrict our discussion to the data for the largest system we simulated ($L=24$).

From Fig. 6, we clearly observe that on the nearest neighbors to the impurity binding site (i.e., for $r=1$), the local

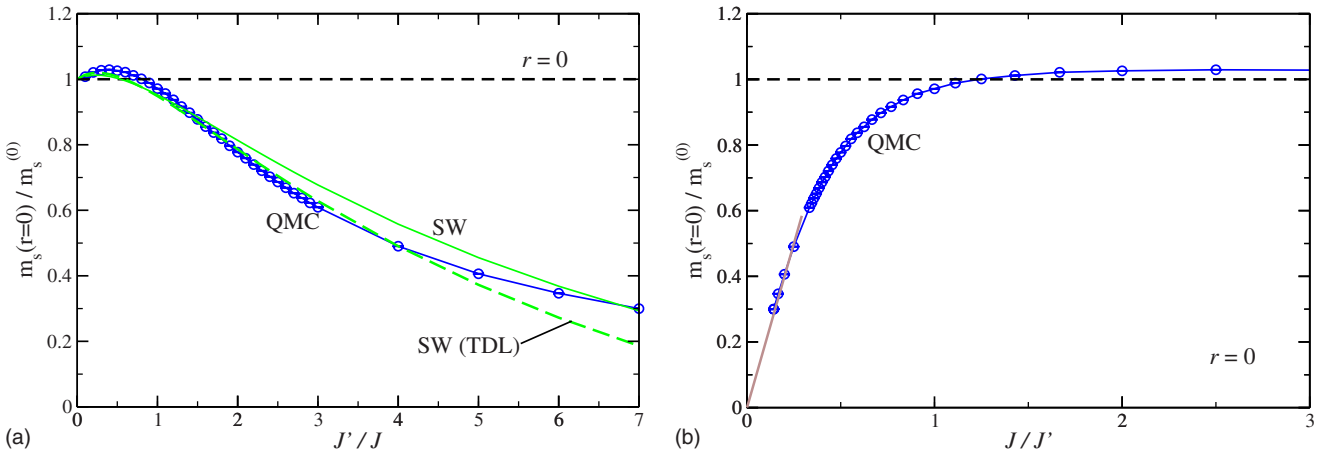

FIG. 5. (Color online) Local staggered magnetization $m_s(r=0)$ from QMC as a function of (a) J'/J and (b) J/J' for the host site at $r=0$ that couples to the impurity spin. The dashed horizontal lines denote the reference value of the clean host system and the other two lines in (a) are the results from spin-wave (SW) theory in the thermodynamic limit (TDL) and for a finite system of $L=24$ sites. Also shown in (b) is a linear extrapolation of the QMC data to the limiting value of 0.

staggered magnetization is enhanced for any finite value of $J'>0$ as expected. However, as seen from the same figure, $m_s(r=1)$ exhibits a maximum value near $J'/J\approx 1.5$ before converging from above toward the asymptotic value in the static impurity limit. In order to exhibit the approach toward the limiting values more directly, we plot in Figs. 5(b) the behavior of $m_s(r)$ as a function of J/J' for $r=0$, $r=1$, $r=\sqrt{2}$, and $r=2$, respectively. For $r=0$, our data are consistent with the results from Ref. 6 that the decoupling of the binding spin from the reminder of the host occurs only in the limit $J'/J\to\infty$. For other values of r, the quantum Monte Carlo data also show the expected scaling for small values of J/J' to the limiting value from the static vacancy case. Furthermore, the observed behavior is consistent with a linear approach at low values of J/J'. This is indicated in Figs. 5(b) by linear extrapolation lines.

The variation of the local staggered magnetization upon increasing J' leads to a corresponding change in the spin-spin correlation function. In particular, we consider the correlation between a spin in the vicinity of the impurity and a spin located far away from the impurity site. In the thermodynamic limit, this distant spin can be considered to reside at $r=\infty$, whereas on the finite lattices accessible to quantum Monte Carlo simulations, we take the most distant spin available, accounting for the periodic boundary conditions. The corresponding spin-spin correlation function is denoted by $C(r)$, where r is the distance of the spin near the impurity to the impurity binding site. Furthermore, we denote by $C^{(0)}(r)$ the value of this correlation on the clean lattice (i.e., for $J'=0$). In the thermodynamic limit, the value of the local staggered magnetization at $r=\infty$ does not change due to the single impurity, i.e., $m_s(\infty)=m_s^{(0)}$, so that $C(r)=m_s(r)m_s^{(0)}$ and hence the normalized correlation function $C(r)/C^{(0)}(r)=m_s(r)/m_s^{(0)}$ equals the normalized local magnetization. Figure 9 shows the quantum Monte Carlo data for the normalized correlation function at different values of r in the vicinity of the impurity as a function of J'/J. The correlation function $C(r)$ shows the expected behavior,

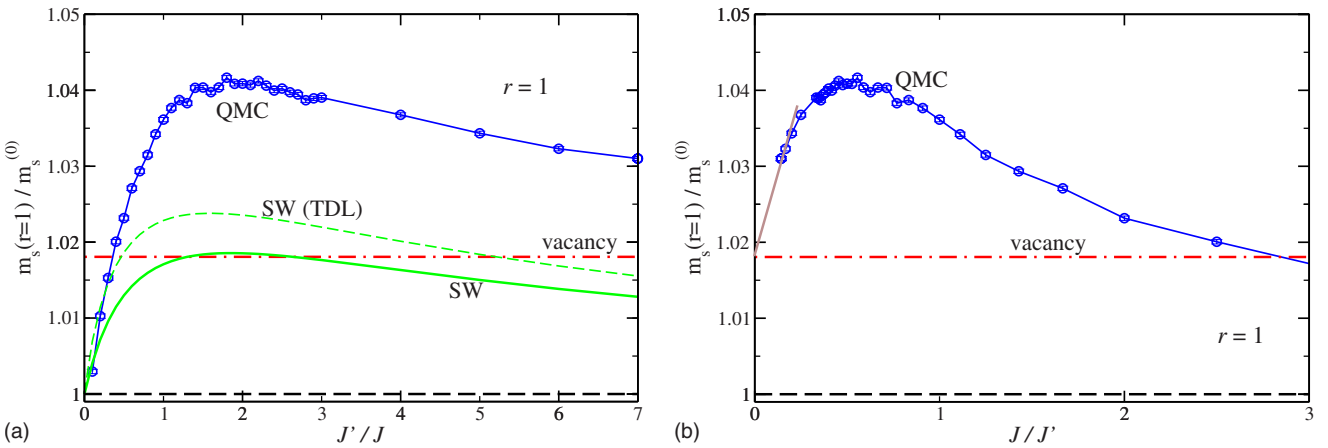

FIG. 6. (Color online) Local staggered magnetization $m_s(r=1)$ from QMC as a function of (a) J'/J and (b) J/J' for host sites at $r=1$. The dashed horizontal lines denote the reference value of the clean host system and the dotted-dashed line represents the limiting value for $J'/J\to\infty$, corresponding to a nonmagnetic impurity (vacancy). The other two lines in (a) are the results from SW theory in the TDL and for a finite system of $L=24$ sites. Also shown in (b) is a linear extrapolation of the QMC data to the limiting value.

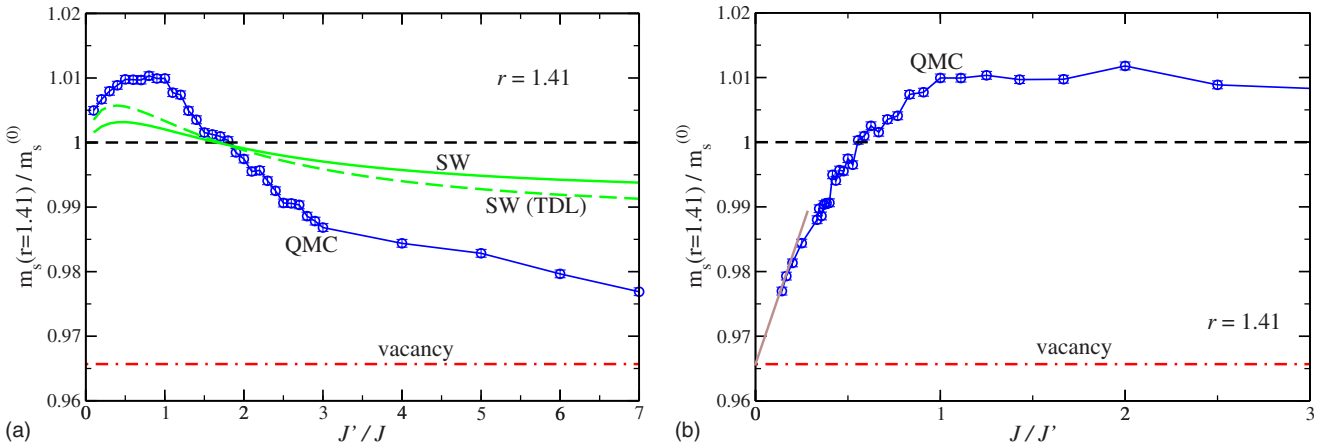

FIG. 7. (Color online) Local staggered magnetization $m_s(r=\sqrt{2})$ from QMC as a function of (a) J'/J and (b) J/J' for host sites at $r=\sqrt{2}$. The dashed horizontal line denotes the reference value of the clean host system and the dotted-dashed line represents the limiting value for $J'/J\to\infty$, corresponding to a nonmagnetic impurity (vacancy). The other two lines in (a) are the results from SW theory in the TDL and for a finite system of $L=24$ sites. Also shown in (b) is a linear extrapolation of the QMC data to the limiting value.

in that it traces closely the behavior of the local staggered magnetization $m_s(r)$, i.e., an impurity-enhanced antiferromagnetism for weak J'/J and the eventual reduction for $r\neq 1$ toward the value in the vacancy limit.

In Ref. 12, the deviation of the local staggered magnetization from the value in the clean case has been calculated within a perturbative approach based on spin-wave theory. The resulting change in the local staggered magnetization at a site at position $\mathbf{r}$ with respect to the impurity binding site is given by

$$m_s(\mathbf{r}) - m_s^{(0)} = \frac{2J'}{SN^2}\sum_{\mathbf{p},\mathbf{q}} \frac{C_{\mathbf{p},\mathbf{q}} e^{i(\mathbf{p}-\mathbf{q})\cdot\mathbf{r}}}{D_{\mathbf{p},\mathbf{q}}}, \tag{8}$$

where $S=1/2$ in the current case and both $\mathbf{p}$ and $\mathbf{q}$ are summed over the first magnetic Brillouin zone. For a site on the same sublattice as the impurity binding site at $r=0$,

$$C_{\mathbf{p},\mathbf{q}} = 2J' u_{\mathbf{q}}^2 v_{\mathbf{p}}^2 \omega_{\mathbf{q}} - J' u_{\mathbf{p}}^2 u_{\mathbf{q}}^2 (\omega_{\mathbf{p}} + \omega_{\mathbf{q}}) + 8J u_{\mathbf{q}}^2 v_{\mathbf{p}}^2 \omega_{\mathbf{p}} \omega_{\mathbf{q}},$$

and on the other sublattice

$$C_{\mathbf{p},\mathbf{q}} = -8J u_{\mathbf{p}} u_{\mathbf{q}} v_{\mathbf{p}} v_{\mathbf{q}} \omega_{\mathbf{p}} \omega_{\mathbf{q}}.$$

Here,

$$u_{\mathbf{q}} = \sqrt{\frac{1}{2\omega_{\mathbf{p}}} + \frac{1}{2}}, \quad v_{\mathbf{q}} = -\,\mathrm{sgn}(\gamma_{\mathbf{q}}) \sqrt{\frac{1}{2\omega_{\mathbf{p}}} - \frac{1}{2}},$$

with $\omega_{\mathbf{p}}=\sqrt{1-\gamma_{\mathbf{q}}^2}$ and $\gamma_{\mathbf{q}}=\frac{1}{2}(\cos q_x+\cos q_y)$ and for both sublattices

$$D_{\mathbf{p},\mathbf{q}} = (\omega_{\mathbf{p}} + \omega_{\mathbf{q}})(J' + 4J\omega_{\mathbf{p}})(J' + 4J\omega_{\mathbf{q}}).$$

In the above, we corrected for a minor mistake in the equation for $C_{\mathbf{p},\mathbf{q}}$ given in Ref. 12.

We compare in Figs. 5(a) the quantum Monte Carlo results to this spin- wave estimate of the local staggered magnetization for various distances r. We show results from the

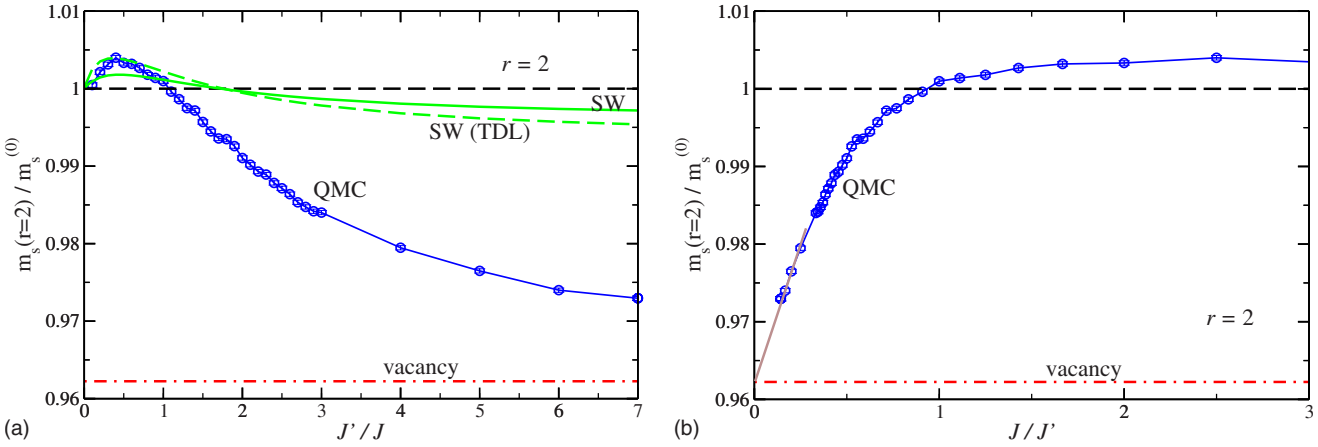

FIG. 8. (Color online) Local staggered magnetization $m_s(r=2)$ from QMC as a function of (a) J'/J and (b) J/J' for host sites at $r=2$. Dashed horizontal line denotes the reference value of the clean host system and dotted-dashed line represents the limiting value for $J'/J\to\infty$, corresponding to a nonmagnetic impurity (vacancy). The other two lines in (a) are the results from SW theory in the TDL and for a finite system of $L=24$ sites. Also shown in (b) is a linear extrapolation of the QMC data to the limiting value.

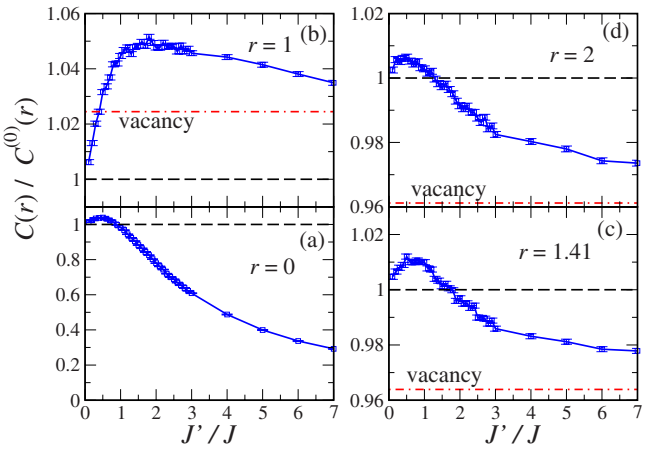

FIG. 9. (Color online) Spin-spin correlations between a site at a distance r from the impurity binding site and the most distant spin on the $L=24$ square lattice with periodic boundary conditions as a function of J'/J for (a) $r=0$, (b) $r=1$, (c) $r=\sqrt{2}$, and (d) $r=2$. Dashed horizontal lines denote the reference value of the clean host system and dotted-dashed lines represent the limiting values for $J'/J \to \infty$, corresponding to a nonmagnetic impurity (vacancy).

spin-wave theory for a finite lattice with $L=24$, as well as values after an extrapolation to the thermodynamic limit (TDL), obtained from a fit of finite-size data up to $L=100$ to a polynomial up to second order in the inverse system size. We find that the analytical prediction compares qualitatively well to the quantum Monte Carlo results. In particular, the spin-wave theory traces the crossover behavior of the staggered magnetization from the initial increase to the eventual decrease for $r \neq 1$, as well as the different behavior at $r=1$. Comparing the analytical data for the TDL and $L=24$, small finite-size effects are visible, which however do not follow the same trend for different values of J'/J [compare, e.g., the behavior in Fig. 7(a) for $J'<J$ to the one for $J'>2J$]. In general, it appears that finite-size effects are less pronounced in the vicinity of the crossover from enhanced toward reduced local staggered magnetization. With respect to a quantitative comparison, it is interesting to note, that instead of a maybe expected general overestimation of antiferromagnetic order by the spin-wave approach, we also find cases, where the analytical prediction underestimates the local staggered magnetization. This is seen most prominent in Fig. 5(a) for the sites at $r=1$, in particular in the regime where $J'>J$. Quantum fluctuations on the stronger J' bond, reducing an antiferromagnetic alignment of the impurity spin with its binding host spin, apparently help to stabilize the alignment with the host antiferromagnetism next to the binding site.

IV. CONCLUSIONS

In summary, we employed quantum Monte Carlo simulations to study the evolution of the staggered magnetization profile in an ordered quantum antiferromagnet on the square lattice with respect to a finite antiferromagnetic coupling of a single host spin to an impurity spin. We observed a broad crossover region, around $J' \approx 1.5\ J$, below which the antiferromagnetism is enhanced within the host, whereas beyond this regime, the enhancement gets restricted to the nearest neighbors of the impurity binding site. Since it depends on the location of a spin within the host, below which value of J' the local staggered magnetization is enhanced, no distinct crossover coupling J' exists in this setup. Merely, the behavior crosses from one regime to the other within a finite range around $J' \approx 1.5\ J$. The approach of the static vacancy limit is found to be consistent with a linear in the coupling ratio J/J'. The behavior of the local staggered magnetization is qualitatively well described by a recently presented perturbative approach based on spin-wave theory.[12] Within a finite-size study, one cannot exclude that even for weak J', the observed enhancement of the antiferromagnetism will not extend over the whole lattice in the thermodynamic limit. However, the observed good agreement with the analytical results provides strong support for the global enhancement found within the spin-wave theory approach. According to this approach, the change in the local staggered magnetization as induced by the impurity crosses over from a decay $\propto 1/r$ at intermediate distances to $\propto 1/r^3$ at large distances.[12] In the future, it would be interesting to perform a similar analysis also for other magnetically ordered systems, e.g., on the honeycomb lattice, where larger quantum fluctuations emerge due to the reduced coordination of the lattice structure or the triangular lattice, where however, different numerical methods need to be applied due to the severe quantum Monte Carlo sign problem on this geometrically frustrated lattice. It would also be interesting to probe competing order parameters, such as bond order, in models of two-dimensional quantum antiferromagnets closer to a quantum critical point and analyze their response to a magnetic impurity of varying coupling strength, similar to the recent study on static vacancies.[26]

ACKNOWLEDGMENTS

We thank M. Barbosa da Silva Neto, A. Lüscher, and Zi Yang Meng for helpful discussions and acknowledge the allocation of CPU time on the HLRS Stuttgart and NIC Jülich supercomputers.

[1] A. H. Castro Neto, E. Novais, L. Borda, G. Zarand, and I. Affleck, Phys. Rev. Lett. **91**, 096401 (2003).
[2] S. Sachdev, J. Stat. Phys. **115**, 47 (2004).
[3] N. Nagaosa, Y. Hatsugai, and M. Imada, J. Phys. Soc. Jpn. **58**, 978 (1989).
[4] J. Igarashi, K. Murayama, and P. Fulde, Phys. Rev. B **52**, 15966 (1995).
[5] K. Murayama and J. Igarashi, J. Phys. Soc. Jpn. **66**, 1157 (1997).
[6] V. N. Kotov, J. Oitmaa, and O. Sushkov, Phys. Rev. B **58**, 8495 (1998).

[7] V. Y. Irkhin, A. A. Katanin, and M. I. Katsnelson, Phys. Rev. B **60**, 14779 (1999).
[8] S. Sachdev and M. Vojta, Phys. Rev. B **68**, 064419 (2003).
[9] K. H. Höglund and A. W. Sandvik, Phys. Rev. Lett. **91**, 077204 (2003).
[10] O. P. Sushkov, Phys. Rev. B **68**, 094426 (2003).
[11] K. H. Höglund and A. W. Sandvik, Phys. Rev. B **70**, 024406 (2004).
[12] A. Lüscher and O. P. Sushkov, Phys. Rev. B **71**, 064414 (2005).
[13] E. Manousakis, Rev. Mod. Phys. **63**, 1 (1991).
[14] A. W. Sandvik, Phys. Rev. B **56**, 11678 (1997).
[15] A. W. Sandvik and H. G. Evertz, arXiv:0807.0682 (unpublished).
[16] N. Bulut, D. Hone, D. J. Scalapino, and E. Y. Loh, Phys. Rev. Lett. **62**, 2192 (1989).
[17] A. W. Sandvik, E. Dagotto, and D. J. Scalapino, Phys. Rev. B **56**, 11701 (1997).
[18] G. B. Martins, M. Laukamp, J. Riera, and E. Dagotto, Phys. Rev. Lett. **78**, 3563 (1997).
[19] S. Wessel, A. Jagannathan, and S. Haas, Phys. Rev. Lett. **90**, 177205 (2003).
[20] A. Jagannathan, R. Moessner, and S. Wessel, Phys. Rev. B **74**, 184410 (2006).
[21] T. Koma and H. Tasaki, Phys. Rev. Lett. **70**, 93 (1993).
[22] T. Koma and H. Tasaki, Commun. Math. Phys. **158**, 191 (1993).
[23] S. Wessel and I. Milat, Phys. Rev. B **71**, 104427 (2005).
[24] A. W. Sandvik, Phys. Rev. B **59**, R14157 (1999).
[25] P. Henelius and A. W. Sandvik, Phys. Rev. B **62**, 1102 (2000).
[26] R. K. Kaul, R. G. Melko, M. A. Metlitski, and S. Sachdev, Phys. Rev. Lett. **101**, 187206 (2008).